JCEC
THE JOURNAL OF ENGINEERING AND EXACT SCIENCES

OPEN ACCESS

The Journal of Engineering and Exact Sciences – jCEC, Vol. 09 N. 11 (2023)
journal homepage: https://periodicos.ufv.br/jcec
eISSN: 2527-1075
ISSN: 2446-9416

Analysis and simulation of turbulent flow around an immersed body with constant temperature using the Immersed Boundary Method

Análise e simulação do escoamento turbulento entorno de um corpo imerso com temperatura constante pelo Método da Fronteira Imersa

Article Info:
Article history: Received 2023-09-20 / Accepted 2023-10-04 / Available online 2023-10-04
doi: 10.18540/jcecvl9iss11pp16664-01e

Rômulo Damasclin Chaves dos Santos
ORCID: https://orcid.org/0000-0002-9482-1998
Department of Physics, Technological Institute of Aeronautics, São Paulo, Brazil
E-mail: damasclin@gmail.com
Jorge Henrique de Oliveira Sales
ORCID: https://orcid.org/0000-0003-1992-3748
State University of Santa Cruz – DCEX, Brazil
E-mail: jhosales@uesc.br

Resumo
Neste estudo, apresentamos um método de fronteira imersa para analisar interações entre fluidos e corpos em escoamentos bidimensionais (2D) em torno de geometrias complexas, com foco na transferência de calor e turbulência. O método utiliza uma malha Euleriana para o fluido, e outra malha Lagrangiana para o corpo imerso, assegurando condições de ausência de deslizamento e considerando trocas de calor. Usamos equações de Navier-Stokes e da energia com modelos de turbulência Smagorinsky (LES) e Spalart-Allmaras (URANS). Um código computacional foi implementado para calcular coeficientes de sustentação, arrasto e Nusselt, comparando os resultados com estudos anteriores em diferentes números de Reynolds. Essa pesquisa avança na compreensão das interações fluido-corpo em geometrias complexas e na termofluidodinâmica.
Palavras-chave: Método da Fronteira Imersa. Convecção Mista. Escoamento Turbulento.

Abstract
In this study, we present an immersed boundary method to analyze interactions between fluids and bodies in two-dimensional (2D) flows around complex geometries, focusing on heat transfer and turbulence. The method uses an Eulerian grid for the fluid, and another Lagrangian grid for the immersed body, ensuring conditions of no slip and considering heat exchanges. We use Navier-Stokes and energy equations with Smagorinsky (LES) and Spalart-Allmaras (URANS) turbulence models. A computational code was implemented to calculate lift, drag and Nusselt coefficients, comparing the results with previous studies at different Reynolds numbers. This research advances the understanding of fluid-body interactions in complex geometries and thermofluid dynamics.
Keywords: Immersed Boundary Method. Mixed Convection. Turbulent Flow.

1. Introduction

In this study, we address the mathematical modeling of fluid mechanics phenomena using the conservation equations for fluid properties, specifically momentum, mass (continuity), and energy conservation. These equations describe the forces acting on the fluid and energy exchanges in different regions of the flow. We employ the finite difference method to discretize these equations for incompressible Newtonian fluids, relating viscous stress terms to deformation rates in the velocity field, enabling us to simulate flow dynamics through the Navier-Stokes equations.

Traditional domain discretization methods pose challenges in terms of implementation and computational time, requiring successive remeshing for each iteration, along with the introduction of a new generalized coordinate system. To overcome these physical and mathematical challenges, we've developed a computational code for the immersed boundary methodology in thermofluid interaction. This study builds upon key references, such as the works of Badr & Dennis (1985) and Badr *et al*. (1990), addressing heat transfer around rotating cylinders.

Additionally, we present the immersed boundary methodology developed by Park *et al*. (2017) for fluid-body interactions with heat transfer, utilizing Eulerian and Lagrangian grids to define fluid and temperature fields as well as body movement. Momentum and heat-transfer between Eulerian and Lagrangian variables are addressed using the Dirac delta function.

Furthermore, Santos, R.D.C *et al*. (2018) introduced the immersed boundary methodology coupled with a virtual physical model to simulate two-dimensional flows around a heated square cylinder. Results demonstrate that the influence of the heated surface increases with Reynolds number.

This study investigates heat-transfer and turbulence in complex geometries with surrounding fluids. Numerical results are consistent and align with previous findings in the literature

2. Formulation for the fluid motion and temperature

According to the work of Santos, R.D.C *et al*. (2018) and Santos, R.D.C. dos, & Sales, J.H.O. (2023), considering an incompressible and two-dimensional flow a Newtonian fluid, with a domain represented by Ω, and a boundary represented by $\partial\Omega$, with the surface of the immersed body being heated with constant temperature, which can be modeled through discretized points, previously named by Lagrangian points. Since the effect of the frontier is taken into account through the introduction of the forcing term in the momentum and energy equation, the equations that describe the heat transfer by mixed convection in the immersed boundary methodology are expressed as follows

$$\nabla . \mathbf{u} = 0 , \tag{1}$$

$$\rho_0 \left[\frac{\partial \mathbf{u}}{\partial t} + (\mathbf{u}.\nabla)\mathbf{u}\right] = -\nabla p + \mu\nabla^2\mathbf{u} + \mathbf{f} , \tag{2}$$

$$\rho_0 \left[\frac{\partial \mathbf{u}}{\partial t} + (\mathbf{u}.\nabla)\mathbf{u}\right] = -\nabla p + \mu\nabla^2\mathbf{u} + \rho_{\mathbf{0}}\mathbf{g}[1 - \beta(T - T_\infty)]\mathbf{j} + \mathbf{f} , \tag{3}$$

$$\rho_0 c_p \left[\frac{\partial T}{\partial t} + (\mathbf{u} . \nabla)T\right] = k\nabla^2 T + q , \tag{4}$$

where Eqs. (1), (2) and (4) are forced convection, while Eqs. (1), (3) and (4) are for natural convection, and in Eq. (3), the Boussinesq approximation is used. The terms, **u,** p, T and T_∞ denote, velocity vector, pressure, temperature and reference temperature, respectively. The terms, ρ_0, μ, β, k and c_p are fluid density at temperature $T = T_\infty$, viscosity, thermal diffusivity, thermal expansion coefficient and specific heat at constant pressure, **g** is a downward gravitational acceleration; the term $\rho_{\mathbf{0}}\mathbf{g}\big(1 - \beta(T - T_\infty)\big)$ accounts for the effects of the fluid temperature on the fluid flow, the term **j** is the unit vector in the positive y-axis direction, respectively.

The term of force **f** and thermal source q in the Eqs. (2) e (3) are the Euler force fields where these sources model the existence of the interface immersed in the flow, visualizing the body immersed in the flow having non-null value in Eulerian grid near the Lagrangian grid, being expressed by

$$\mathbf{f}(x,t) = \int_{\partial\Omega_b} F(\mathbf{X}_k,t)\delta(x-\mathbf{X}_k)d\mathbf{X}_k\,, \tag{5}$$

where, $F(\mathbf{X}_k,t)$ is the Lagrangian force density, calculated on the interface points x and $\mathbf{X}_k$ which are the positions of a particle of Eulerian and Lagrangian fluid on the interface, respectively. The term $\delta(x-\mathbf{X}_k)$ is the Dirac delta function, which represents the interaction between the fluid and the immersed boundary. Similarly, the thermal source represented by q is added to Eq. (4), being responsible for making the flow feel the presence of the heated solid interface, in other words, it is heating source at the Lagrangian point on the immersed border, being able to be expressed by

$$q(x,t) = \int_{\partial\Omega_b} Q(\mathbf{X}_k,t)\delta(x-\mathbf{X}_k)d\mathbf{X}_k\,, \tag{6}$$

where, $Q(\mathbf{X}_k,t)$ is the heat flux at the border being the difference between the derivative of the approximate specific temperature.

2.1 Calculation of forces acting on discrete points

The methodology developed and implemented calculates the forces that act at the discrete points of a given boundary, as well as determining the so-called interfacial force or Lagrangian force. The characterization of the Lagrangian force represents the difference between the various immersed boundary methodologies. In this work, only the rigid boundaries were treated (no elasticity), but the model can be used or extended to other types of interfaces, for example, for elastic boundaries, boundaries between different fluids, etc. The model uses the diffusion of interfacial forces on the interior of the flow. Thus, the Eulerian force field is applied in the vicinity of the immersed boundary, and its value is minimized as the distance to the interface increases. This model dynamically assesses not only the force that the fluid exerts on the solid surface immersed in the flow, bur takes into account the thermal exchange between them.

The Lagrangian force $F(\mathbf{X}_k,t)$, and the thermal source $Q(\mathbf{X}_k,t)$, are evaluated separately, in other words, for Lagrangian force a balance of amount of movement was carried out on a fluid particle that in close to the fluid-solid interface, while for the thermal part, the dimensionless energy equation was applied, which shows the interaction between the particle fluid and the interface, which takes into account all the terms of the Navier-Stokes equation. Then, assuming that all particle fluid, including those over the interface, must satisfy the balance of amount of movement and energy. Thus, the density of interfacial force can be evaluated using the principle of conservation of the momentum and energy, applying over any participle of fluid that makes up the flow. Therefore, taking the particle fluid crossing an arbitrary immersed boundary interface, we obtain the following formulation

$$F(\mathbf{X}_k,t) = \underbrace{\rho\frac{\partial\mathbf{U}(\mathbf{X}_k,t)}{\partial t}}_{F_a} + \underbrace{\rho\,\nabla[\mathbf{U}(\mathbf{X}_k,t)\mathbf{U}(\mathbf{X}_k,t)]}_{F_i} + \underbrace{\nabla p(\mathbf{X}_k,t)}_{F_p} - \underbrace{\mu\nabla^2(\mathbf{X}_k,t)}_{F_v}\,, \tag{7}$$

where, the portions referring to the terms of the Eq. (7), from left to right, are called acceleration force, inertial force, pressure force and viscous force, respectively.

In a manner similar to that performed in Eq. (7), for the calculation of the thermal source in the particle fluid in contact with the interface, an energy balance is performed as follows

$$Q(\mathbf{X}_k, t) = \frac{\partial \Theta(\mathbf{X}_k, t)}{\partial \mathrm{t}} + \nabla[\mathbf{U}(\mathbf{X}_k, t)\Theta\mathbf{U}(\mathbf{X}_k, t)] - \frac{1}{Pe}\nabla^2\Theta(\mathbf{X}_k, t)\,, \tag{8}$$

where, the portions referring to Eq. (8), from de right, are called local temperature variation rate, thermal dissipation rate due to convection and diffusive thermal energy transport rate. In Eq. (8), each term is evaluated based on the values of the variables (velocity, pressure and temperature), of the Eulerian grid, interpolated for the Lagrangian grid and for the auxiliary points used in obtaining spatial derivatives. This process is detailed in the next subsection.

2 .2 Calculation of velocity, pressure and temperature

2.2.1 Auxiliary point allocation process

The first step is to arbitrate an initial Lagrangian point for calculating the interfacial force $F(\mathbf{X}_k, t)$. Then, two mutually orthogonal auxiliary lines are drawn on this point, one of which is parallel to one of the Eulerian axes. Two auxiliary points are marked on each of the lines, on the outside of the solid body, at a distance Δx and $2\Delta x$ of the Lagrangian point considered. This distance is necessary in order to prevent two auxiliary points from being allocated within the same Eulerian cell. The grids that are more that $2\Delta x$ distance from the Lagrangian points, do not contribute to the interpolation. The internal and external regions of the solid body were identified with the aid of the normal unitary vector on the surface, which has its positive direction forcing outside the immersed body. The auxiliary points are always located in the regions of interest of the flow, that is, in the region to be simulated. Thus, the values of velocity, pressure and temperature at the points, in general, are not know, but can be obtained, from neighboring cells, with the ais of a distribution/interpolation function.

Thus, the general equation for obtaining the velocity at Lagrangian points and auxiliary points is expressed in the following formula

$$\mathbf{U}(\mathbf{X}_k) = \sum_i D_i(x_i - \mathbf{X}_k)\,\mathbf{U}(x_i)\,, \tag{9}$$

where, $\mathbf{U}(\mathbf{X}_k)$ are the Lagrangian velocities, calculated at the auxiliary points and at the point $\mathbf{X}_k$ by the interpolation of the Eulerian velocities. Similarly, for the calculation of pressure and temperature derivatives at each Lagrangian point, it was necessary to obtain the pressure and temperature values on the interface, at point $\mathbf{X}_k$.

Thus, for the calculation of pressure and temperature an auxiliary point, which is in a normal position at a distance Δx from the Lagrangian point. The general equation for obtaining the pressure and temperature at the auxiliary points or on the interface and at the Lagrangian points in the x and y directions are given, respectively, by the systems

$$\begin{cases} p(\mathbf{X}_k) = \sum_i D_i(x_i - \mathbf{X_k})\, p(x_i) \\ \Theta(\mathbf{X}_k) = \sum_i D_i(x_i - \mathbf{X_k})\, \Theta(x_i) \end{cases} \tag{10}$$

$$\begin{cases} p(\mathbf{Y}_k) = \sum_i D_i(x_i - \mathbf{Y_k})\, p(y_i) \\ \Theta(\mathbf{Y}_k) = \sum_i D_i(x_i - \mathbf{Y_k})\, \Theta(y_i) \end{cases} \tag{11}$$

where, $p(\mathbf{X}_k)$ and $p(\mathbf{Y}_k)$ are pressure values on the interface, and $p(x_i)$ and $p(y_i)$ are pressure value in the nearest Eulerian grids, in the x and y directions, respectively. Similarly, $\Theta(\mathbf{X}_k)$ and $\Theta(\mathbf{Y}_k)$ are the temperatures at auxiliary points at k points and $\Theta(\mathrm{x}_i)$, the temperature at the nearest Eulerian points. The distribution/interpolation function D, adopted in thus work, is used for the interpolation of variables in the Eulerian grid. Regarding the computational cost involved, it was reduced when

considering non-null D for distances less than $2\Delta x$ from the interpolation point, which is also valid for the $F(\mathbf{X}_k, t)$ distribution. Therefore, in this work, Peskin (1977) proposal, modified by Juric (1996), is used, being defined by

$$D(x - \mathbf{X_k}) = \prod_{m=1}^{N} \frac{g(r_x)g(r_y)}{h^2} , \tag{12}$$

where,

$$g(r) = \begin{cases} g_1(r) & , if \quad \|r\| < 1 \\ 0.5 - g_1(2 - \|r\|) & , if \quad 1 < \|r\| < 2 \\ 0 & , if \quad \|r\| > 2 \end{cases} \tag{13}$$

where, $g_1(r) = {}^1\!/_8 \left(3 - 2\|r\|\sqrt{1 + 4\|r\| - 4\|r\|^2}\right)$, and r is called the radius of influence of the distribution function, being represented here by $\left[\frac{1}{h}(x - x_k)\right]$ or $\left[\frac{1}{h}(y - y_k)\right]$. The term, $h = \Delta x = \Delta y$, is the size of the Eulerian grid and (x, y) the coordinates of a Eulerian point in the domain. To calculate the temperature at each time step in the iterative process over the immersed boundary, the following equation was used

$$\Theta(\mathbf{X}_k) = \sum_i D_i(x_i - \mathbf{X}_k)\, \Theta(x_i) . \tag{14}$$

Thus, after the interpolation of velocity, pressure and temperature at the interface and at auxiliary points, the derivatives that make up the terms for the calculation of Lagrangian source terms are determined in the x and y directions, with the so-called Lagrange polynomials of first and second order. Generically, denominated the components of velocity or pressure, defined by the interpolation function ϕ, given by the linear combination of the Lagrange polynomials, in the form

$$\phi(x) = \sum_{i=0}^{m} \phi_i \prod_{j=0, j\neq i}^{m} \frac{x - x_j}{x_i - x_j} . \tag{15}$$

2.2.2 Calculation of Lagrangian force distribution and thermal source

After calculating the terms das Eqs. (7) and (8), and obtaining the values for $F(\mathbf{X}_k, t)$ and $Q(\mathbf{X}_k, t)$, then the Eulerian terms are calculated for $\mathbf{f}$ and q. The system calculation for the terms $\mathbf{f}$ and q, in the x and y direction, are presented below, respectively

$$\begin{cases} \mathbf{f}(x_i) = \sum_i D_i\, (x_i - \mathbf{X}_k)\, F(\mathbf{X_k})\, \Delta s\, (\mathbf{X}_k) \\ \mathrm{q}(x_i) = \sum_i D_i\, (x_i - \mathbf{X}_k)\, Q(\mathbf{X_k})\, \Delta s\, (\mathbf{X}_k) \end{cases} \tag{16}$$

and

$$\begin{cases} \mathbf{f}(y_i) = \sum_i D_i\, (y_i - \mathbf{Y}_k)\, F(\mathbf{Y_k})\, \Delta s\, (\mathbf{Y}_k) \\ \mathrm{q}(y_i) = \sum_i D_i\, (y_i - \mathbf{Y}_k)\, Q(\boldsymbol{Y_k})\, \Delta s\, (\mathbf{Y}_k) \end{cases} \tag{17}$$

where, in the Eqs. (16) and (17), in the respective x and y directions, $\mathbf{f}(x_i)$ and $\mathbf{f}(y_i)$, are the forces at each Eulerian node, while $F(\mathbf{X_k})$ and $F(\mathbf{Y_k})$, are the force in each Lagrangian node being

distributed to Eulerian nodes. The terms, $\mathrm{q}(x_i)$ and $\mathrm{q}(y_i)$, is presented are heat sources for each Eulerian node, due the presence of immersed heated, and $Q(\mathbf{X_k})$ and $Q(\mathbf{Y_k})$ are the thermal source in each Lagrangian node being distributed to the nodes Eulerian, thus forming, a thermal field of Eulerian force that acts on the fluid particles near the border.

3. Mathematical models

3.1 The Smagorinsky model

According to the work of Santos, R.D.C *et al*. (2018) and Santos, R.D.C. dos, & Sales, J.H.O. (2023), the algebraic modeling Smagorinsky (1963) is based on the local equilibrium hypothesis for small scales, so that the injected energy in the spectrum, defined by

$$\xi = -\overline{u'_i u'_j S_{ij}} = 2\nu\overline{S_{ij}}\,\overline{S_{ij}}\,, \tag{18}$$

equals the dissipated energy by the viscous effects. The terms, u'_i and u'_j are, respectively, the characteristics scales of velocity of the sub-grid. It is assumed that the turbulent viscosity sub-grid is proportional to these characteristics' scales, according to the equation

$$\nu_t = C_s \ell \left(u'_j u'_i\right)^{\frac{1}{2}}. \tag{19}$$

The turbulent viscosity, Eq. (19), can be expressed as a function of the strain rate tensor (S_{ij}), the characteristic length scale (ℓ), associated with the grid size and the C_s constant, called the Smagorinsky constant, the viscosity turbulent is then represented by

$$\nu_t = (C_s \ell)^2 \sqrt{2\bar{S}_{ij}\bar{S}_{ij}}\ , \tag{20}$$

where, the strain rate tensor $\bar{S}_{ij}$ is represented by

$$\bar{S}_{ij} = \frac{1}{2}\left(\frac{\partial \bar{u}_i}{\partial x_j} + \frac{\partial \bar{u}_j}{\partial x_i}\right), \tag{21}$$

where, the implementation related to the damping function was implemented in such a way as to dampen the turbulent viscosity close to the walls of the immersed boundary, regardless of the type of geometry to be considered.

3.2 The Spalart-Allmaras model

The Spalart-Allmaras turbulence model emerged in the 1990's after a coherent convergence between ideas about an empirical model that resolved the turbulence, that is, that which only a single equation, the modeling would occur directly, solving the question of the main turbulent parameter: turbulent viscosity, without involving calculations with turbulent energy or dissipation or vorticity, where in other existing models, these characteristic parameters are necessary to define the turbulence behavior in the flow. In the Spalart-Allmaras model, a transport equation for turbulent viscosity is established, using empiricism and argument from dimensional analysis, invariance and a selective dependence on molecular viscosity, according to the works of Spalart *et al*. (1992). The equation includes a non-viscous destruction term that depends on the distance to the wall. Unlike algebraic models, the first models of an equation are local, in the sense that the equation at one point does not depend on the solution at other points. Therefore, it is compatible with grids of any nature. The solution close to the wall is less difficult to obtain.

Wall and undisturbed flow conditions are elementary. The model produces relatively smooth turbulent laminar transition at points specified by the user. The model was calibrated in boundary

layers with a pressure gradient. The turbulent viscosity (v_t) is calculated from the Spalart-Allmaras working aid variable, $\tilde{v}$, and damped by the function f_{v_i} near to the walls,

$$v_t = \tilde{v}\, f_{v_1}\,, \tag{22}$$

where,

$$f_{v_1} = \frac{\chi^3}{\chi + C_{v_1}^3}, \tag{23}$$

with,

$$\chi = \frac{\tilde{v}}{v}. \tag{24}$$

Thus, the so-called auxiliary work variable of the Spalart-Allmaras model, $\tilde{v}$, obeys the following transport equation

$$\begin{aligned}\frac{\partial \tilde{v}}{\partial t} + \frac{\partial}{\partial x_j}\left(u_j \tilde{v}\right) &= c_{b_1}\left(1 - f_{t_2}\right)\tilde{S}\tilde{v} + \frac{1}{\sigma}\left[\frac{\partial}{\partial x_j}\left((v + \tilde{v})\frac{\partial \tilde{v}}{\partial x_j}\right) + c_{b_2}\frac{\partial \tilde{v}}{\partial x_j}\frac{\partial \tilde{v}}{\partial x_j}\right] \\ &\quad - \left[c_w f_w - \frac{c_{b_1}}{k^2} f_{t_2}\right]\left[\frac{\tilde{v}}{d_w}\right]^2 + f_{t_1}\Delta U^2\,,\end{aligned} \tag{25}$$

where the terms on the right side of Eq. (25) represent, respectively: (**i**) the production of turbulent viscosity, (**ii**) the molecular and turbulent diffusions of $\tilde{v}$, (**iii**) the dissipation of $\tilde{v}$, (**iv**) the destruction of $\tilde{v}$ that reduces the turbulent viscosity to the wall and, finally, (**v**) the terms that model transition effects to turbulence, indicated by the subindex t. For regions distant from the walls, the function f_{v_i} has no influence on the calculation of turbulent viscosity, being its unit value and, therefore, making $v_t = \tilde{v}$. The production term of the transport equation, Eq. (25), also needs a correction near to the wall, which is performed by replacing the parameter *S* with a modified variable $\tilde{S}$, which is also influenced by a damping function f_{v_2}, defined similarly to f_{v_2}. Thus, $\tilde{S}$ and f_{v_2} are presented below by following formulation

$$\tilde{S} = S + \frac{\tilde{v}}{(k d_w)^2}\, f_{v_2}\,, \tag{26}$$

$$f_{v_2} = 1 - \frac{\chi}{1 + \chi f_{v_1}}, \tag{27}$$

where, d_w, Eq. (26), is the distance to the near wall, and *S* is the modulus of the strain rate, calculated with the variables of the filtered field, being calculated by

$$S = \sqrt{2\bar{S}_{ij}\bar{S}_{ij}}\,. \tag{28}$$

The function f_w is defined as a unit value for the region of the logarithmic boundary layer, intensifying the term of distribution as it approaches the wall, tending to zero for the most distant regions of the wall, thus being defined as being

$$f_w = g\left(\frac{1+c_{w_3}^6}{g^6+c_{w_3}^6}\right), \tag{29}$$

where,

$$g = r + c_{w_2}(r^6 - r)\,, \tag{30}$$

and,

$$r \equiv \frac{\tilde{v}}{\overline{S}\,k^2 d_w^2}\,. \tag{31}$$

Others constants of the model are $\sigma = {}^{2}/_{3}$, $c_{b_1} = 0.1355$, $c_{b_2} = 0.622$, $k = 0.41$, $c_{w_1} = {}^{c_{b_1}}/_{k^2} + {}^{(1+c_{b_2})}/_{\sigma}$, $c_{w_2} = 0.3$, $c_{w_3} = 2$ and $c_{v_1} = 7.1$. These constants were determined empirically. Regarding the average energy equation with turbulent diffusivity, applying an additional scale Q_j, being represented by

$$\frac{\partial\overline{\Theta}}{\partial t} + \frac{\partial\left(\bar{u}_j\overline{\Theta}\right)}{\partial x_i} = \frac{\partial}{\partial x_j}\left[\alpha\left(\frac{\partial\overline{\Theta}}{\partial x_j}\right) + \overline{u_j\Theta} - \bar{u}_j\overline{\Theta}\right], \tag{32}$$

where, the term $\overline{\Theta}$ is the resolved temperature field.

5. Numerical method

The numerical method used in this paper is the fractional steps that unites the velocity and pressure. With the aim to solve the Navier-Stokes equation, result new velocity and pressure fields. For the time discretization is used Euler's method of the first order. The Navier-Stokes equation were solved explicitly. The correction of pressure results in a linear system, solved by Modified Strongly Implicit Procedure developed by Schneider & Zedan (1981). The Eq. (2), can be rewritten in the following in the following way

$$\frac{u_i^{n+1} - u_i^m}{\Delta t} + \left[\frac{\partial}{\partial x_j}\left(u_i^n u_j^n\right)\right] = -\frac{1}{\rho}\frac{\partial p^{n+1}}{\partial x_i} + \frac{\partial}{\partial x_j}\left[(v+v_t)\left(\frac{\partial u_i^n}{\partial x_j} + \frac{\partial u_j^n}{\partial x_i}\right)\right] + f_i^n\,. \tag{33}$$

In the fractional step method, the velocities, pressure and the forcing term of the predictive instant (n) are used to calculate, in the predictive step, and estimate for the velocity in the current time $\bar{u}_i^{n+1}$, represented by the equation

$$\frac{\bar{u}_i^{n+1} - u_i^m}{\Delta t} + \left[\frac{\partial}{\partial x_j}\left(u_i^n u_j^n\right)\right] = -\frac{1}{\rho}\frac{\partial p^{n+1}}{\partial x_i} + \frac{\partial}{\partial x_j}\left[(v+v_t)\left(\frac{\partial u_i^n}{\partial x_j} + \frac{\partial u_j^n}{\partial x_i}\right)\right] + f_i^n\,, \tag{34}$$

the next step in the fractional step method is to subtract Eq. (34) from Eq. (33), resulting in

$$\frac{\bar{u}_i^{n+1} - u_i^n}{\Delta t} = \frac{1}{\rho}\frac{\partial}{\partial x_i}(p^{n+1} - p^n)\,, \tag{35}$$

doing some algebraic manipulations, we get the pressure field calculated, we obtaining the equation corrected for the velocity in the current iteration (corrector step), being represented by

$$u_i^{n+1} = \bar{u}_i^{n+1} - \frac{\Delta t}{\rho} \frac{\partial p'^{n+1}}{\partial x_i}. \quad (36)$$

6. Results

Using the immersed boundary method coupled virtual physical model, implemented in C++ code, is possible perform simulation of (2D) (two-dimensional) flows around a heated body immersed in the flow. In this section, the flow around a pair of heated circular cylinders in tandem have equal diameters and the same center-to-center distance (L_{CC}). The fluid and the heat flow are characterized by Reynolds number $Re = \frac{\rho U_\infty D}{\mu}$ and Prandtl number $Pr = \frac{\mu c_p}{k}$, where ρ is the fluid density, U_∞ is the free stream velocity, D is the cylinder diameter, μ is the dynamic viscosity, c_p is heat at constant pressure and k the thermal diffusivity. In this work, numerical simulations are conducted for different Reynolds numbers $(Re = 1 - 500)$, while keeping the Prandtl number fixed at $Pr = 0.7$. Both heat and fluid flow characteristics like the drag C_d and lift C_ℓ coefficients, recirculation behind the cylinder, streamline and isotherm pattern, average Nusselt number on the cylinder surface are presented and compared with previous result in the literature. In this case, the angle formed by the segment joining the centers of the two cylinders and the axis of the abscissa is zero.

6.1 Description of the problem and boundary conditions

In the Fig. 1, the two cylinders are identical and fixed with the same diameters, maintained in "tandem" (cylinders in line) with downstream of the cylinder A. The cylinders are confined to a channel with free flow, with uniform velocity (U_∞) and constant temperature $\left(T_c(> T_\infty)\right)$. The horizontal and vertical spacing between the cylinders are fixed in $L_u = 16.5\, d$ and $L_d = 19.5\, d$, respectively. These values are chosen to reduce the effect of boundary conditions on the inlet and outlet relative to the flow patter and the cylinder boundary.

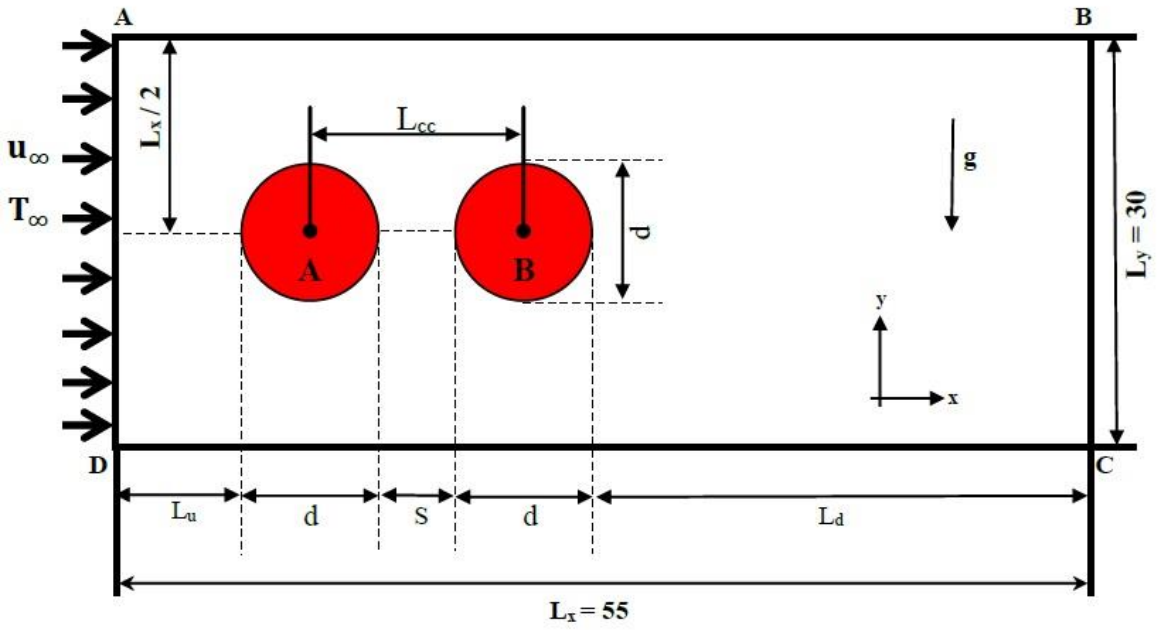

Figure 1: Illustration of the computational domain with two cylinders in tandem configuration.

The drag (C_d) and lift (C_ℓ) coefficients for the calculation of each cylinder are performed as follows

$$C_d = C_{dp} + C_{dv} = \frac{2F_d}{\rho U_\infty^2 D}, \tag{37}$$

$$C_\ell = C_{\ell p} + C_{\ell v} = \frac{2F_\ell}{\rho U_\infty^2 D}, \tag{38}$$

where, $C_{\ell p}$ and $C_{\ell v}$ represent the lift coefficients due pressure and viscous forces, respectively. In a similar way, C_{dp} and C_{dv}, represent the drag coefficients due to the pressure and viscous forces. The terms, F_d and F_ℓ are forces of drag and lift, respectively, acting on the surface of the cylinder. Thus, the drag and lift coefficients can be obtained from the expressions:

$$\begin{cases} C_{dp} = 2\int_0^1 (p_f - p_r)\, dy\,, \\ C_{dv} = \dfrac{2}{Re}\int_0^1 \left[\left\{\left(\dfrac{\partial u}{\partial y}\right)_s + \left(\dfrac{\partial u}{\partial y}\right)_i\right\} dx + \left\{\left(\dfrac{\partial u}{\partial x}\right)_f + \left(\dfrac{\partial u}{\partial x}\right)_r\right\} dy\right], \end{cases} \tag{39}$$

$$\begin{cases} C_{lp} = 2\int_0^1 (p_i - p_s)\, dy\,, \\ C_{\ell v} = \dfrac{2}{Re}\int_0^1 \left[\left\{\left(\dfrac{\partial u}{\partial y}\right)_f + \left(\dfrac{\partial u}{\partial y}\right)_b\right\} dx + \left\{\left(\dfrac{\partial u}{\partial x}\right)_t + \left(\dfrac{\partial u}{\partial x}\right)_i\right\} dy\right], \end{cases} \tag{40}$$

6.2 Flow fields for $Re = 500$ and $Ri = 0$ in cylinders in tandem with forced convection

The Fig. (2) present simplified fields of effective viscosity, vorticity, isothermal lines, and aerodynamics coefficients, C_d and C_ℓ, for the flow around cylinder tandem, for Reynolds and Richardson numbers, equals to 500 and 0, respectively.

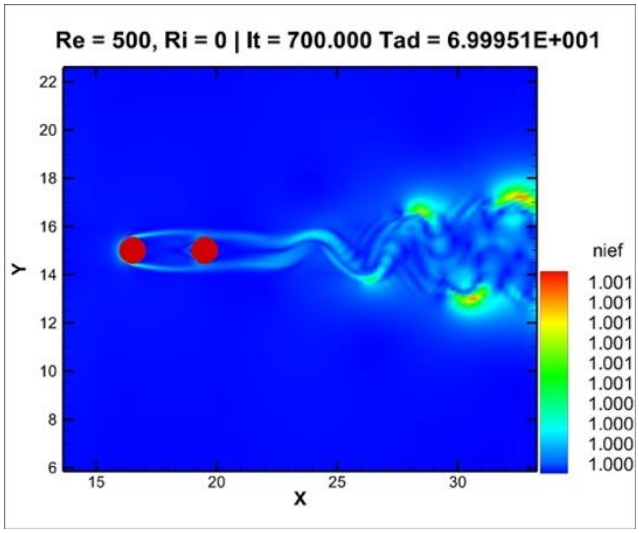

(a)

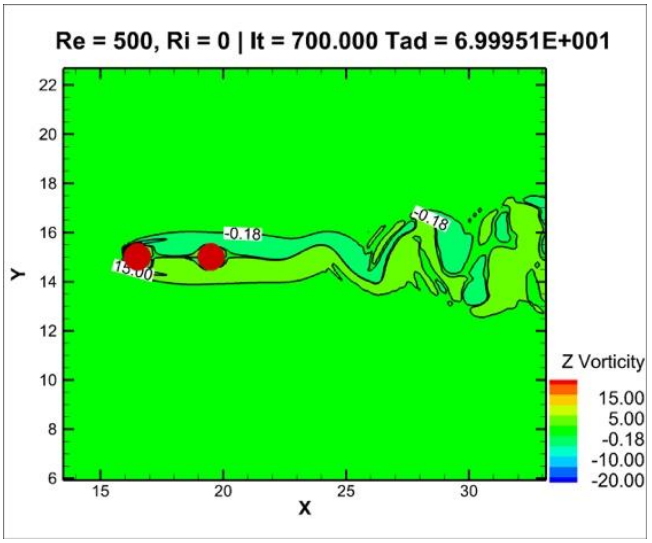

(b)

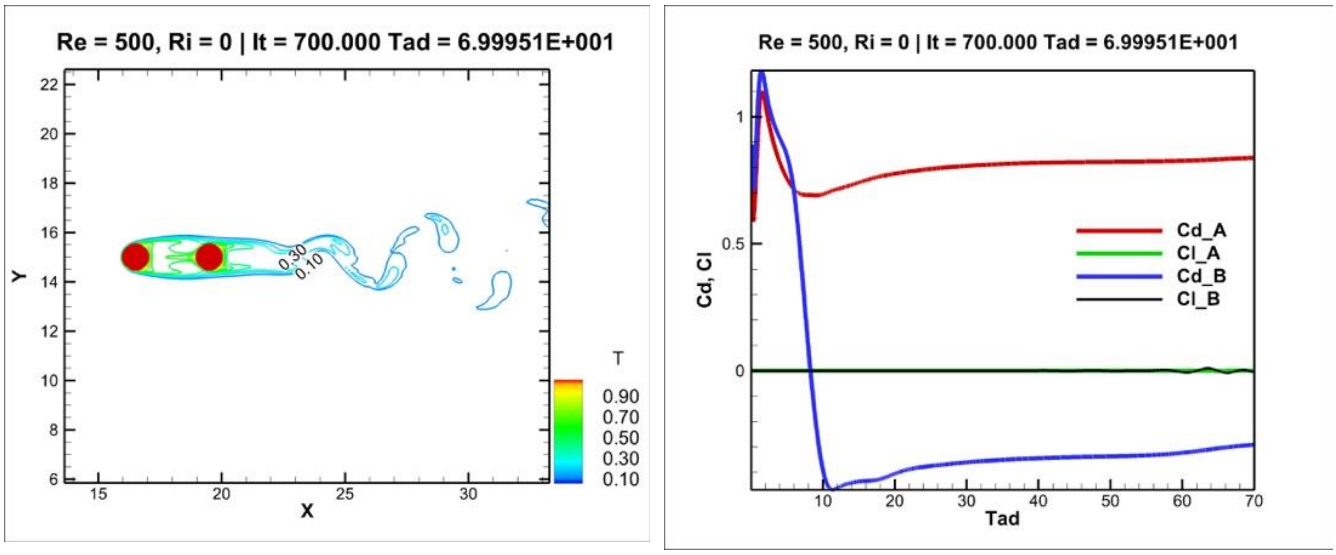

(c) (d)

Figure 2: Spalart-Almarras model for simplified fields of effective viscosity (a) vorticity (b); isotherms lines (c) and Drag (C_d) and Lift C_ℓ coefficients for cylinders, for $Re = 500$ with $Ri = 0$.

The main results for the simulations can be summarized as follows:

- A wake forms upstream of the second cylinder, but it needs to be checked whether it can be decreased or suppressed with the increase of the distance between the cylinders;
- The isothermal lines reflect the same behavior of the pattern of the streamlines (current lines);
- The average Nusselt number increase for $Re = 500$ for different value of Ri, even keeping the distance between the cylinders;
- The thermal buoyancy is suppressed in the recirculation zones of the tandem cylinders, even with a mounting angle;
- The thermal buoyancy tends to in the recirculation zones of the tandem cylinders, even with a mounting angle;
- The thermal buoyancy tends to increase the coefficient of drag and the average Nusselt number of the cylinder more than the second.

6.3 Variations of the Nusselt number

One of the main purposes of the heat transfer calculations involving cylinders is to determine the local and total transfer around isothermal cylinders. The effect of the flow, especially with respect to the heat transfer, can be better observed by analyzing the local heat transfer coefficient, also known as the Nusselt local number. In the Fig. (3), for different Richardson numbers, the distributions of Nusselt numbers along the perimeter of the upstream and downstream cylinders are provided. For $L_{cc}/d = 3$, $Re = 100$, $Re = 200$ and $Re = 500$, for different Richardson numbers, the local distributions of the Nusselt numbers along the perimeter of the upstream and downstream cylinders are provided. For $L_{cc}/d = 3$, although the local profile of the Nusselt number of the upstream cylinder is similar to that of an isolated cylinder, the downstream cylinder has completely different characteristics, as the transfer rate is closely related to the flow, the local minimum rates of heat transfer appear at the front back stagnation points of the downstream cylinder, where the magnitude of velocities are relatively small.

This, in Fig. (3-(a)), the maximum heat transfer from the downstream cylinder is exhibited with a double protuberance in $\theta \approx 57°$ and $\theta \approx 265°$ from the cylinder wall, where thermal layers (also known as thermal plumes) and hydrodynamics becomes thinner. The formation of vortices in the downstream region of the cylinder coincides with the oscillations of the average Nusselt number from large amplitude to low amplitude during a vortex release period for $L_{cc}/d = 3$ and $Re = 500$ for different values of Ri, as see in Fig. (3-(b)). It is important to note that although the Nusselt's local distribution of the downstream cylinders resembles that of the upstream cylinder, typified as large protuberance, its magnitude is smaller than of the upstream cylinder, indicating smaller heat-to-cylinder conversion to downstream.

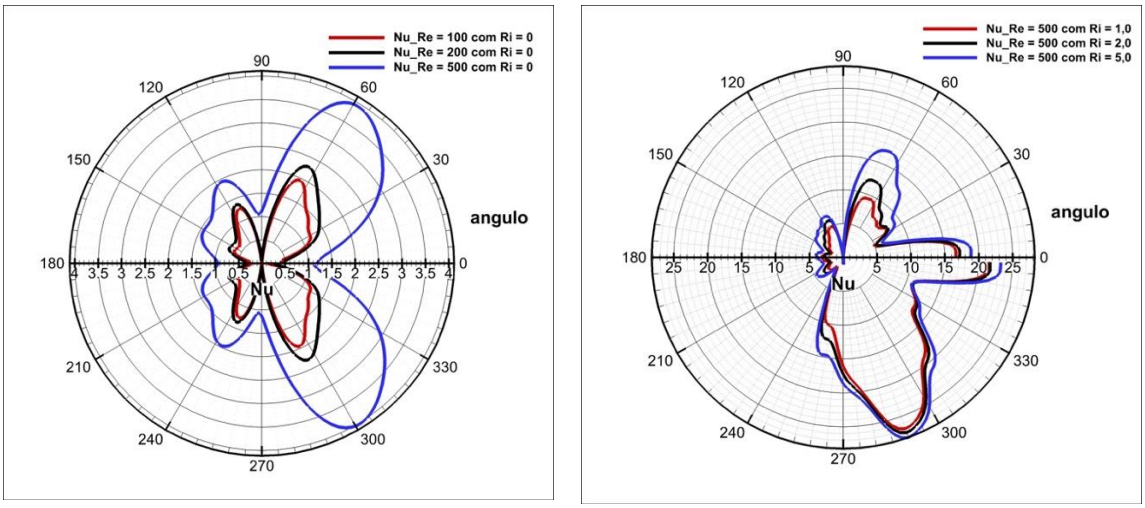

(a) (b)

Figure 3: Local variation of the Nusselt number to the same dimensionless instants: (a) $Re = 100$, $Re = 200$ and $Re = 500$ for $Ri = 0$; and (b) $Re = 500$ for $Ri = 1.0, Ri = 2.0$ and $Ri = 5.0$.

7. Conclusion

In this study, we introduced an advanced boundary-condition-enforced immersed boundary method developed for simulating heat and mass transfer problems. The influence of thermal boundaries on flow and temperature fields was effectively incorporated through velocity and temperature corrections. The temperature correction process is handled implicitly, ensuring that the temperature at the immersed boundary, derived from the corrected temperature field, adheres to the physical boundary conditions. To account for momentum transfer between the immersed body and the surrounding fluid, we implemented an additional momentum forcing term within the fluid-body equation. However, we chose to present only the results of simulations related to the Spalart-Allmaras Model, which is part of the Unsteady Reynolds-Averaged Navier-Stokes (URANS) concept, incorporating a single transport equation for turbulence viscosity, calibrated within pressure gradient layers. This choice allowed us to focus our analysis on the Spalart-Allmaras Model, providing a more detailed and specific insight into the obtained results. To facilitate our research, we developed a computational code to implement the mentioned methodology, enabling us to comprehensively analyze the interaction of heat transfer phenomena within turbulence in thermofluid dynamics interactions around complex isothermal geometries. The excellent agreement of our results with available literature data underscores the validity and reliability of our numerical approach.

References

Badr, H. M., & Dennis, S. C. R. (1985). Time-dependent viscous flow past an impulsively started rotating and translating circular cylinder. *Journal of Fluid Mechanics,* 158, 447-488. https://ui.adsabs.harvard.edu/link_gateway/1985JFM...158..447B/doi:10.1017/S0022112085002725

Badr, H. M., Coutanceau, M., Dennis, S. C. R., & Menard, C. (1990). Unsteady flow past a rotating circular cylinder at Reynolds numbers 10^3 and 10^4. *Journal of Fluid Mechanics,* 220, 459-484. https://doi.org/10.1017/S0022112090003342

Juric, D., Computation of Phase Change, Ph. D. Thesis, Mech. Eng. *Univ. of Michigan,* USA, 1996. https://www.osti.gov/servlets/purl/537364

Park, S. G., Chang, C. B., Kim, B. and Sung, H. J. (2017). Simulation of Fluid-Flexible Body Interaction with Heat Transfer. *Int. J. Heat Mass Transfer,* 110, 20–33. https://doi.org/10.1016/j.ijheatmasstransfer.2017.03.012

Peskin, C. S. Numerical Analysis of Blood Flow In The Heart. *Journal of Computational Physics.* v.25, pp. 220-252, 1977. https://doi.org/10.1016/0021-9991(77)90100-0

Schneider, G. E.; Zedan, M. (1981). A Modified Strongly Implicit Procedure for the Numerical Solution of Field Problems. *Numerical Heat Transfer,* v. 4, n.01, pp. 1-19, 1981. https://doi.org/10.1080/01495728108961775

Smagorinsky, J. (1963) General Circulation Experiments with the Primitive Equations: I. The Basic Experiment. *Monthly Weather Review,* 91, 99–164. http://dx.doi.org/10.1175/1520-0493(1963)091<0099:GCEWTP>2.3.CO;2

Spalart, P. & Allmaras, S. (1992). A One-Equation Turbulence Model for Aerodynamics Flows. *Recherce Aeropatiale,* No. 1, 5–21. https://turbmodels.larc.nasa.gov/Papers/RechAerosp_1994_SpalartAllmaras.pdf

Santos, R. D., Gama, S.M., & Camacho, R. G. (2018). Two-Dimensional Simulation of the Navier-Stokes Equations for Laminar and Turbulent Flow around a Heated Square Cylinder with Forced Convection. *Applied Mathematics,* 9(03), 291–312. 10.4236/am.2018.93023

Santos, R.D.C. dos, & Sales, J.H.O. (2023). Turbulent Flow Analysis with Banach and Sobolev Spaces in the LES Method Incorporating the Smagorinsky Subgrid-Scale Model. *The Journal of Engineering and Exact Sciences*, *9*(10), 16534–01e. https://doi.org/10.18540/jcecvl9iss10pp16534-01e

Santos, R. D. C. dos, & Sales, J. H. de O. (2023). Treatment for regularity of the Navier-Stokes equations based on Banach and Sobolev functional spaces coupled to anisotropic viscosity for analysis of vorticity transport. The Journal of Engineering and Exact Sciences, 9(8), 16656–01e. https://doi.org/10.18540/jcecvl9iss8pp16656-01e